



Article

# Polymer Composites of Low-Density Polyethylene (LDPE) with Elongated Hematite ( $\alpha$ -Fe<sub>2</sub>O<sub>3</sub>) Particles of Different Shapes

Ljerka Kratofil Krehula <sup>1,\*</sup>, Ana Peršić <sup>1</sup>, Nina Popov <sup>2</sup> and Stjepko Krehula <sup>2</sup>

<sup>1</sup> Faculty of Chemical Engineering and Technology, University of Zagreb, Marulićev Trg 19, 10000 Zagreb, Croatia; apersic@fkit.unizg.hr

<sup>2</sup> Division of Materials Chemistry, Ruđer Bošković Institute, Bijenička 54, 10000 Zagreb, Croatia; npopov@irb.hr (N.P.); krehul@irb.hr (S.K.)

\* Correspondence: krehula@fkit.unizg.hr

**Abstract:** Due to the intensive search for new types of advanced polymer materials for targeted applications, this work offers insight into the properties of low-density polyethylene/hematite composites. The specific feature of this study lies in the use of elongated hematite particles of different shapes. Uniform ellipsoid-, peanut- and rod-shaped hematite particles were hydrothermally synthesized and incorporated into the polymer matrix of low-density polyethylene (LDPE). LDPE/hematite composites are prepared by melt mixing. Hematite particles are characterized by scanning electron microscopy (SEM) and powder X-ray diffraction (PXRD). The pure LDPE polymer and LDPE/hematite composites were studied by FT-IR and UV-Vis-NIR spectroscopy and by thermogravimetric analysis (TGA). The determination of the mechanical and barrier properties was also carried out. The obtained results indicate the influence of the elongated particles on the improvement of LDPE properties. An increase in thermal stability and UV-absorption was observed as well as the improvement of mechanical and barrier properties. The improvement of the composites' properties in comparison to the pure LDPE is especially visible in the composites prepared with low content of hematite (0.25%). LDPE/hematite composites have promising characteristics for application as packaging materials with enhanced mechanical, thermal and barrier properties as well as UV-protective materials.

**Keywords:** polymer composites; low-density polyethylene; hematite; elongated particles; particle shape; thermal stability; mechanical properties; barrier properties; UV protection



**Citation:** Kratofil Krehula, L.; Peršić, A.; Popov, N.; Krehula, S. Polymer Composites of Low-Density Polyethylene (LDPE) with Elongated Hematite ( $\alpha$ -Fe<sub>2</sub>O<sub>3</sub>) Particles of Different Shapes. *J. Compos. Sci.* **2024**, *8*, 73. <https://doi.org/10.3390/jcs8020073>

Academic Editor: Francesco Tornabene

Received: 29 December 2023

Revised: 23 January 2024

Accepted: 7 February 2024

Published: 11 February 2024



**Copyright:** © 2024 by the authors. Licensee MDPI, Basel, Switzerland. This article is an open access article distributed under the terms and conditions of the Creative Commons Attribution (CC BY) license (<https://creativecommons.org/licenses/by/4.0/>).

## 1. Introduction

Preparation of polymer composites presents a way to improve polymer materials' properties. The combination of a specific polymer matrix and a certain type of filler results in unique properties of the obtained composite, which is a completely new material. Such material formulation may have improved properties, i.e., better thermal stability, increased mechanical, barrier, UV-blocking or other characteristics, compared to the pure polymer material. Polymer composites have potential to be used as a category of advanced materials with high performance [1,2].

Among various filler types, metal oxides represent very important fillers for polymer composites due to the many benefits brought to the polymer after their incorporation into a polymer matrix. They can contribute to the overall attributes of the composite material due to their outstanding characteristics such as mechanical, magnetic, catalytic, electrical, optical and other properties [3]. Different types of metal oxide particles may be used for such applications: titanium dioxide (TiO<sub>2</sub>), zinc oxide (ZnO), iron oxide, silicon dioxide (SiO<sub>2</sub>), copper oxide (CuO) etc. [4–6]. The combination of polymer and metal oxide represents a special type of material, which can be advanced in many ways, for example, due to high strength-to-weight ratio.

Polymer composites with the iron oxide hematite ( $\alpha\text{-Fe}_2\text{O}_3$ ) are promising non-toxic material systems for the production of packaging, for medical, construction or other applications due to the many good qualities obtained by the presence of hematite, which brings thermal stability, electromagnetic absorption, corrosion resistance and catalytic activity [7]. According to the scientific literature, preparation of polymer composites with hematite included several polymer matrices: polystyrene [8,9], polyacrylonitrile [10], polycaprolactone [11], polyaniline [12] or poly(vinyl-pyrrolidone) [13]. Prepared polymer composites showed several improved properties compared to the pure polymer matrices, i.e., increased mechanical properties [8], better thermal stability [9] or corrosion resistance [14].

This work is part of a comprehensive research that studies the influence of synthesized hematite particles of different sizes and shapes on the properties of polyethylene/hematite composites. To our best knowledge, such a study has not yet been undertaken. The further importance of the complete study is that it encompasses and unites the synthesis of hematite particles and the preparation of polymer composites. The properties of LDPE/hematite composites, with different types of hematite particles (spherical, pseudocubic, ellipsoid-shaped, peanut-shaped and rod-shaped), were intently studied in order to be able to suggest the composite types and compositions which possess the best specific properties and may be used as an improved functional polymer material with a targeted application. The impact of the hematite particles' shape and size as well as its ratio in a polymer composite plays an important role in final material properties.

To our best knowledge, except our previous study [15], there are no studies about the preparation procedures and properties of polyethylene/hematite composites and the influence of hematite on polyethylene polymer matrix. Low-density polyethylene (LDPE) is one of the most important, most produced and most used polymer materials due to its good processability and low cost. It is a material which is not harmful and is completely safe to use. All these characteristics enable its wide application, primarily as a food packaging material. Our previous work [15] studied the effect of the hematite particles' shape and size on the properties of LDPE. LDPE/hematite composites were prepared with three different types of synthesized hematite particles of different shape and size. They had narrow size distributions and well-defined shapes (pseudocubic, ellipsoidal and spherical). The obtained LDPE/hematite composites had improved thermal, optical, mechanical and barrier properties in comparison to the pure low-density polyethylene (LDPE) [15]. It was determined that all studied hematite particles improved the studied properties of LDPE/hematite composites compared to the pure LDPE. Pseudocubic hematite particles showed the best overall impact on the properties of LDPE/hematite composites. They highly contribute to the enhancement of thermal, mechanical and barrier properties, more than spherical and ellipsoidal hematite particles. Pseudocubic particles also significantly improve the UV-blocking properties of the prepared composite material but less than spherical and ellipsoidal hematite particles. The present work deepens insight into the impact of the hematite particles on the properties of LDPE/hematite composites using the specific, elongated particles of a different shape: ellipsoid-, peanut- and rod-shaped. It is very important to point out that all types of studied elongated particles are well defined and fairly uniform. Elongated hematite particles may have specific properties that are considered as highly desirable in various applications [16–19].

Therefore, the present study goes further and presents a new unique contribution to the properties of low-density polyethylene/hematite composites using elongated hematite particles of different shapes. The properties of hematite particles strongly depend on their shape, and, in several studies [16–19], elongated hematite particles showed better specific properties (catalytic, photocatalytic, electrochemical, photoelectrochemical) compared to hematite particles of some other shapes. Also, it was shown that elongated nanoparticles (nanorods), due to their specific geometry, can significantly improve the properties of functional polymer nanocomposites [20]. In the present study, ellipsoidal, peanut-shaped and rod-shaped hematite particles of well-defined shapes and very good uniformity were synthesized and incorporated into a low-density polyethylene matrix. The influence of

the shape and mass fraction of elongated hematite particles on the thermal, mechanical, UV-Vis absorption and barrier properties of the prepared LDPE/hematite composites was investigated. It is important to point out that the preparation of polymer composites with a specific shape, size and proportion of synthesized filler particles can enable the creation of completely new and unique materials with improved and advanced properties for a targeted application.

## 2. Materials and Methods

### 2.1. Preparation of Hematite Particles

Iron(III) chloride hexahydrate ( $\text{FeCl}_3 \cdot 6\text{H}_2\text{O}$ , 97% Alfa Aesar), sodium hydroxide (NaOH, p.a. Kemika), sodium sulphate ( $\text{Na}_2\text{SO}_4$ , anhydrous, p.a. Kemika), 1,2-diaminopropane ( $\text{CH}_3\text{CH}(\text{NH}_2)\text{CH}_2\text{NH}_2$ , 99% Alfa Aesar) and ultrapure (Milli-Q) water were used for the preparation of elongated hematite particles of different shapes. Uniform peanut- and ellipsoid-shaped hematite particles were prepared using a slightly modified method described by Sugimoto et al. [21], while rod-shaped hematite particles were prepared by a slightly modified direct hydrothermal synthesis method described by Li et al. [22]. To prepare peanut-shaped hematite particles (sample HP1), 90 mL of 6 M NaOH aqueous solution was slowly added to 100 mL of magnetically stirred 2.0 M  $\text{FeCl}_3$  aqueous solution placed in a 250 mL polypropylene (PP) bottle. After that, 6 mL of 1 M  $\text{Na}_2\text{SO}_4$  aqueous solution and 4 mL of water were added to the reaction mixture and the stirring was continued for another 10 min. The obtained mixture was heated in a laboratory oven for 8 days at 100 °C, which produced peanut-shaped hematite particles. For preparation of ellipsoidal hematite particles (sample HE2), 45 mL of 6 M NaOH aqueous solution was slowly added to 50 mL of magnetically stirred 2.0 M  $\text{FeCl}_3$  aqueous solution placed in a 125 mL polypropylene (PP) bottle. Then, 1.5 mL of 1 M  $\text{Na}_2\text{SO}_4$  aqueous solution and 1.5 mL of water were added to the reaction mixture and stirring was continued for another 10 min. The obtained mixture was heated in the laboratory oven for 5 days at 100 °C, which produced ellipsoid-shaped hematite particles. For preparation of rod-shaped hematite particles (sample HR1), 10 mL of 2.0 M  $\text{FeCl}_3$  aqueous solution was poured into a thick-walled polytetrafluoroethylene (PTFE) cup with a capacity of 45 mL. Next, 10 mL of 1,2-diaminopropane was added under strong mixing using a magnetic stirrer and the resulting mixture was homogenized for 30 min. The PTFE cup with reaction mixture was put into a Parr model 4744 acid digestion vessel which was then heated in a laboratory oven for 24 h at 180 °C, resulting in the formation of rod-like hematite particles. Solid samples precipitated by all 3 synthesis methods were washed with redistilled water using a centrifuge and dried in air atmosphere at 60 °C.

### 2.2. Preparation of LDPE/Hematite Composites

Composites of low-density polyethylene and hematite were prepared from LDPE granulate (Dow Chemical, Midland, MI, USA) and hydrothermally synthesized ellipsoid-shaped, peanut-shaped and rod-shaped hematite particles (samples HE2, HP1 and HR1). Polymer composites, marked as LDPE/HE2, LDPE/HP1 and LDPE/HR1, were prepared by mixing of LDPE with hematite in a Brabender kneader, at a temperature of 180 °C. The duration of melt mixing was 3 min and the speed of kneading was 45 rpm. The hematite content in the polymer composites was 0.25, 0.5 and 1% (Table 1). After melt mixing, the prepared polymer composites were shaped into the foils (Figure 1) and plates by hydraulic press Dake (model 44-226) at a temperature of 190 °C.

**Table 1.** Composition of the prepared samples.

Sample	LDPE (wt.%)	Hematite (wt.%)
LDPE	100	0.00
LDPE/0.25%HE2	99.75	0.25
LDPE/0.5%HE2	99.50	0.50
LDPE/1%HE2	99.00	1.00
LDPE/0.25%HP1	99.75	0.25
LDPE/0.5%HP1	99.50	0.50
LDPE/1%HP1	99.00	1.00
LDPE/0.25%HR1	99.75	0.25
LDPE/0.5%HR1	99.50	0.50
LDPE/1%HR1	99.00	1.00

**Figure 1.** Photographs of prepared LDPE/hematite composites.

### 2.3. Characterization

The size and shape of the hematite particles used in the preparation of the composites were observed using a JEOL JSM-7000F field emission scanning electron microscope (FE-SEM). Powder X-ray diffraction (PXRD) patterns of the prepared hematite samples were recorded using a Malvern Panalytical Empyrean diffractometer with a copper anode.

A thermogravimetric analyzer TA Instruments Q500 was used to determine the thermal stability of LDPE and of the obtained polymer composites. Test specimens of 10 mg were analyzed in the temperature range from 25 to 800 °C, at a heating rate of 10 °C/min, in the nitrogen stream. The prepared composite samples and pure LDPE were characterized by attenuated total reflectance Fourier-transform infrared spectroscopy (FT-IR) on a Perkin Elmer Spectrum One FT-IR spectrometer using the attenuated total reflectance (ATR) technique, in the range from 4000 to 650  $\text{cm}^{-1}$  with a resolution of 4  $\text{cm}^{-1}$ . Each

sample was scanned four times. A Zwick 1445 universal device was used for determination of the mechanical properties of pure LDPE and of the composites (samples were 100 mm long, 10 mm wide and ~1 mm thick). The stretching speed was 50 mm/min. Diffuse reflectance UV-Vis-NIR spectra of the studied samples were recorded at 20 °C using a Shimadzu UV-3600 UV-Vis-NIR spectrophotometer with an integrating sphere. Barium sulfate (Nacalai Tesque, Kyoto, Japan) was used as a reference material. Water vapor permeability of pure LDPE and of all composite samples was determined using Herfeld's apparatus. It uses a glass container and a metal lid with a circular hole (36 mm in diameter). The glass container was filled with 50 mL of water, the foil of the studied sample (55 mm in diameter) was placed under the metal lid and it was closed. Then, the glass container was placed in a desiccator containing 97% sulfuric acid. The weight of the glass container with the specimen and the water was measured at the beginning of the measurement as well as after 24 h and 48 h.

### 3. Results and Discussion

#### 3.1. Properties of Hematite Particles

The size and shape of hematite particles in the prepared samples can be seen in the scanning electron microscopy (SEM) images shown in Figure 2. These SEM images show the presence of well-defined and fairly uniform hematite particles in all three hematite samples. All three types of particles are more or less elongated, but at the same time, their shapes are very different: ellipsoidal (sample HE2, Figure 2a,b), peanut-shaped (sample HP1, Figure 2c,d) or rod-shaped (sample HR1, Figure 2e,f). High-magnification images of ellipsoidal and peanut-shaped particles (Figure 2b,d) show nanostructured morphologies of these particles. However, nanostructured morphology is not visible in the high-magnification image of the rod-shaped particles (Figure 2f).

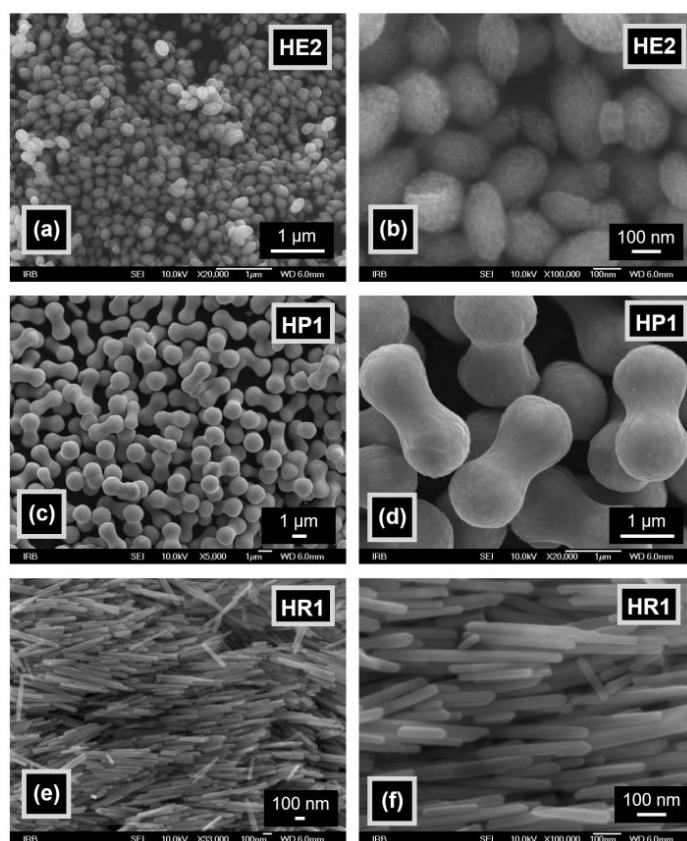


**Figure 2.** Scanning electron microscopy (SEM) images of synthesized ellipsoidal (a,b), peanut-shaped (c,d) and rod-shaped (e,f) hematite particles.

The crystal structure of hematite (trigonal crystal system, space group  $R\bar{3}c$ ) in all three prepared samples was confirmed by recording powder X-ray diffraction (PXRD) patterns (Figure 3). The positions and intensities of the diffraction lines in all three recorded patterns match well with the data given in the standard hematite powder diffraction file (JCPDS card No. 33-0664) shown at the bottom of Figure 3, with no visible additional diffraction lines of other crystalline phases. Very broad diffraction lines in the patterns of samples HE2 and HP1 suggest the presence of very small crystalline grains in these samples, which is in line with the nanostructured morphology observed on the high-magnification SEM images (Figure 2b,d). The average crystallite size was estimated to be 18.9 nm for HE2 and 14.3 nm for HP1 using the line width at half maximum of the strongest diffraction line (104) and the Scherrer equation [23]. In contrast, the diffraction lines in the pattern of sample HR1 are much narrower, indicating much larger crystallites in rod-shaped particles compared to ellipsoidal and peanut-shaped particles, which is also consistent with the absence of nanostructured morphology in the high-magnification SEM image of this sample (Figure 2f).

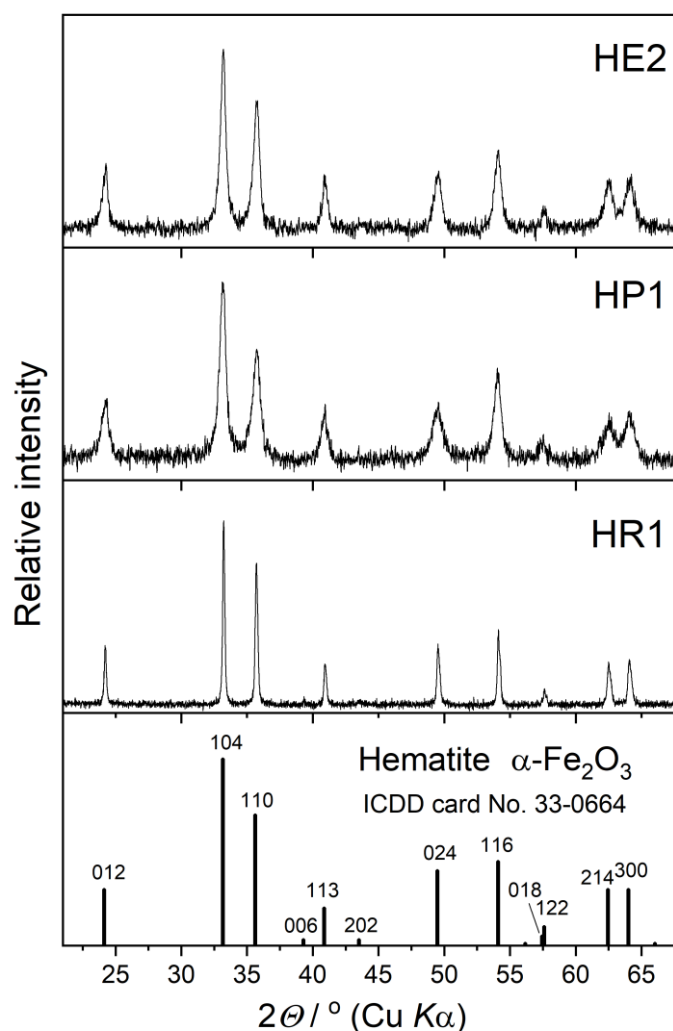


**Figure 3.** Powder X-ray diffraction (PXRD) patterns of synthesized hematite samples.

### 3.2. FT-IR Spectroscopy

FT-IR spectra of pure LDPE polymer and LDPE/hematite composites containing 1 wt.% hematite are shown in Figure 4, where the characteristic absorption peaks for polyethylene are marked. There is a peak for  $\text{CH}_2$  asymmetric stretching at  $2916\text{ cm}^{-1}$  and  $\text{CH}_2$  symmetric stretching at  $2849\text{ cm}^{-1}$ , a peak at  $1460\text{ cm}^{-1}$  for bending deformation and

a maximum at  $719\text{ cm}^{-1}$  for rocking deformation. A weak peak at  $1375\text{ cm}^{-1}$ , representing  $\text{CH}_3$  symmetric deformation [24,25], is also visible. A peak at  $1643\text{ cm}^{-1}$  corresponds to the presence of a stabilizer in LDPE (hindered amine light stabilizer, HALS) [24].

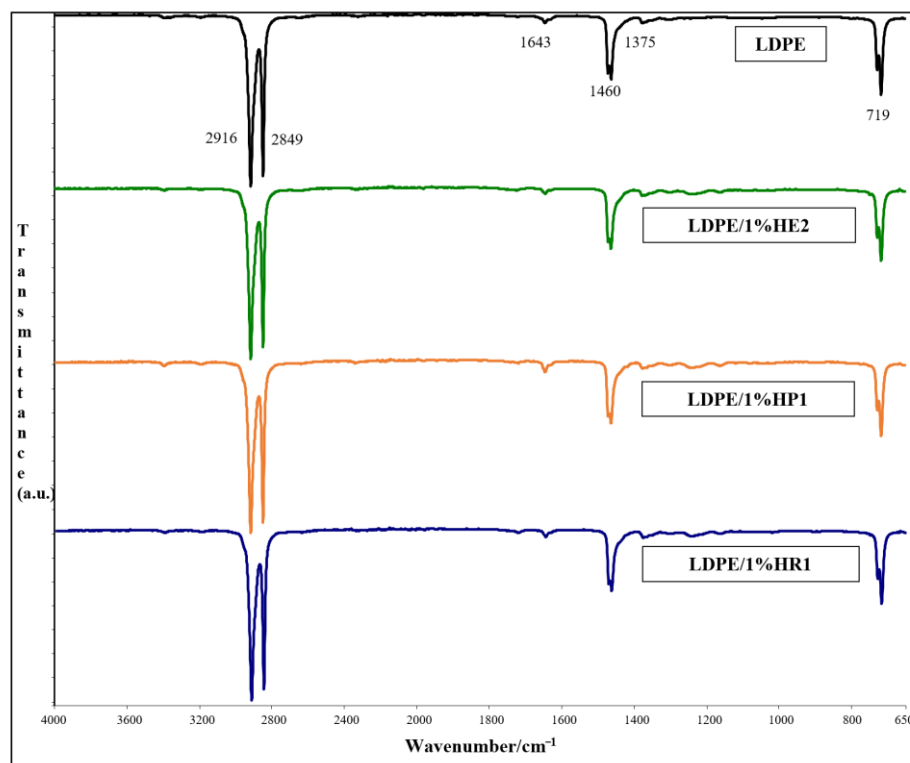


**Figure 4.** Fourier-transform infrared (FT-IR) spectra of prepared LDPE/hematite composites.

A very low content of hematite (1 wt.%) is present in the prepared composites, and it is observed that there are almost no differences between FT-IR spectra of pure LDPE and FT-IR spectra of polymer composites. Furthermore, due to the spectral range of the measurement (from  $4000$  to  $650\text{ cm}^{-1}$ ), peaks for hematite are not observed. Characteristic infrared peaks of hematite are located below  $650\text{ cm}^{-1}$  [26].

It is very important to point out that there is no absorption band characteristic for the formation of carbonyl groups at around  $1720\text{ cm}^{-1}$ , which is a very common and characteristic signal for LDPE degradation [27] which may occur during a material's processing and use.

### 3.3. Mechanical Properties

It is known that fillers can improve the mechanical properties of polymers [1,5]. It is necessary to optimize the preparation procedure for composites in order to avoid filler aggregation and to obtain uniform composite properties. When nanoparticles are used as fillers for polymer material, they can highly influence the composite properties due to their large surface even when they are used in very low quantities [28]. In this work, LDPE/hematite composites are prepared with quite low weight content of hematite: 0.25%, 0.5% and 1%. The results of the measurements of the mechanical properties are presented in Table 2 and in Figures 5 and 6. Figures 5 and 6 show the results of the mechanical properties' measurements for the studied samples expressed as relative tensile strength and relative elongation at break where LDPE is used as a reference material. From the presented results, the improvement of the mechanical properties, compared to pure LDPE polymer, is observed for almost all studied samples.

**Table 2.** Mechanical properties of LDPE and LDPE/hematite composites.

Sample	Tensile Strength (MPa)	Elongation at Break (%)
LDPE	6.98	230.5
LDPE/0.25%HE2	8.56	437.84
LDPE/0.5%HE2	9.58	443.97
LDPE/1%HE2	7.96	435.90
LDPE/0.25%HP1	8.92	461.29
LDPE/0.5%HP1	9.66	461.12
LDPE/1%HP1	9.72	459.15
LDPE/0.25%HR1	9.28	461.56
LDPE/0.5%HR1	7.31	145.01
LDPE/1%HR1	8.05	171.33

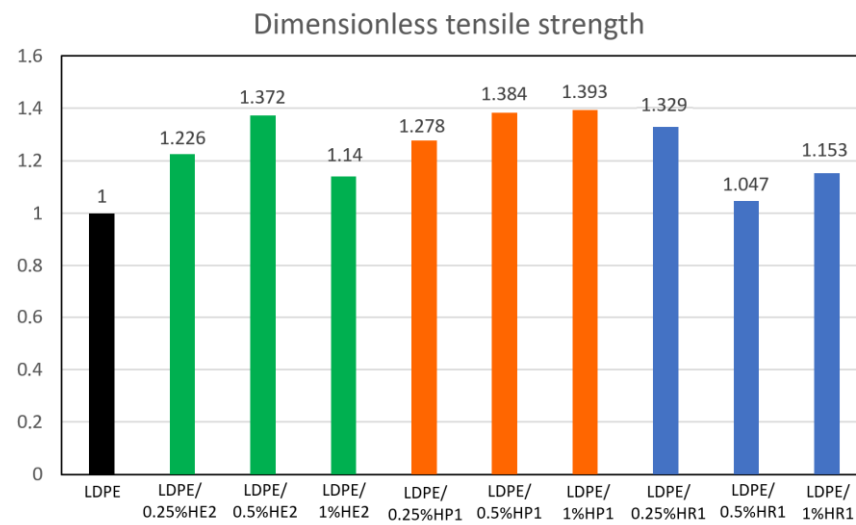


**Figure 5.** Dimensionless tensile strength measured for prepared LDPE/hematite composites.

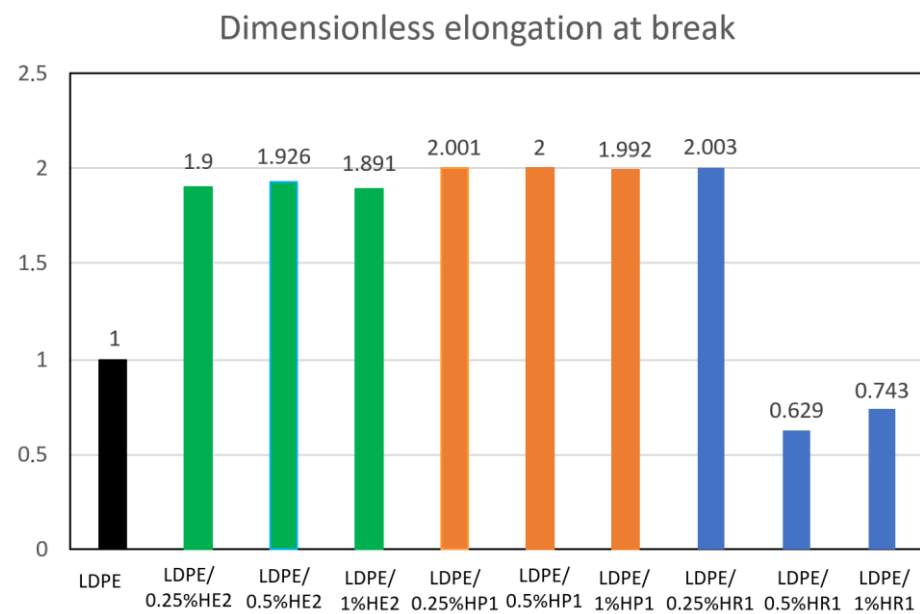


**Figure 6.** Dimensionless elongation at break measured for prepared LDPE/hematite composites.

From the results for tensile strength (Table 2, Figure 5), it can be seen that the values for all studied composites samples are higher than the value for pure LDPE. The highest values are obtained for LDPE/0.5%HP1 and LDPE/1%HP1 composites with the values

of tensile strength for 38.4% and 39.3% higher than the tensile strength of the pure LDPE. It is very important to point out that all three composite samples prepared with very low hematite content (0.25%) show notable improvement of tensile strength, which is higher than the tensile strength of the pure LDPE: for 22.6% in the case of LDPE/0.25%HE2, for 27.8% (LDPE/0.25%HP1) and for 32.9% (LDPE/0.25%HR1). Such results indicate a good dispersion of low hematite filler quantity in an LDPE polymer matrix. It is known that particle loading, particle size and particle/matrix interfacial strength may significantly influence the strength of the composites [29]. If the obtained results for tensile strength are compared to the results obtained in our previous work [15], it can be concluded that the highest values for tensile strength in the present work (LDPE/0.5%HP1 and LDPE/1%HP1) are slightly lower than the highest values in the past paper, which were obtained for the composites with pseudocubic hematite particles. On the other hand, the current values for tensile strength for composites with peanut-shaped hematite particles are quite similar or higher than the tensile strength values for the composites with spherical and ellipsoidal particles in the previous work.

This work studies the influence of elongated but differently shaped hematite particles on the properties of polymer composites. It can be observed that the weakest increase in tensile strength is observed for the samples LDPE/0.5%HR1 and LDPE/1%HR1 due to the use of rod-shaped hematite particles, which show the highest tendency to agglomerate when used in higher content because of their specific geometry and the ability to aggregate. It is known that there is a tendency for rod-like filler nanoparticles to form agglomerates in the surrounding media, which limits the use of such 1D nanofiller types for the reinforcement of polymers [30]. Bogdanović et al. [30] showed that hematite nanofiller has an influence on the improvement of the mechanical properties of an epoxy polymer matrix when the composites are prepared with low filler content (up to 1 wt.%). There is a possibility for the agglomeration of filler particles in the polymer matrix when the filler content exceeds a certain value, which influences the decrease in the mechanical properties [31]. This can be observed for the values of tensile strength for LDPE/1%HE2, LDPE/0.5%HR1 and LDPE/1%HR1 samples. Furthermore, bare filler particles, without surface modification, tend to agglomerate and it is not an easy task to disrupt it during the preparation of polymer composites [32]. However, the procedure for the preparation of polymer composites in this study included mixing of the filler and the polymer before polymer melting. After this step, the mixed polymer and the filler were added to a Brabender kneader and they were there mixed in a melt. By using this mixing procedure, filler is more uniformly distributed in the polymer matrix [33].

Table 2 and Figure 6 present the elongation at break for pure LDPE and for the composite samples. It can be seen that the elongation at break is significantly improved for most samples where the increase in elongation at break from 89% to 100% is observed. The highest values for elongation at break are obtained for all composites prepared with peanut-shaped hematite (HP1) and for the LDPE/0.25%HR1 sample where they are higher for even 100% compared to the pure LDPE. The only exception is the elongation at break for the LDPE/0.5%HR1 and LDPE/1%HR1 samples. Their values are decreased compared to pure LDPE for 37.1 and 25.7, respectively. This suggests that the composites with rod-shaped particles show a decrease in elongation at break as the particle weight content increases due to their already-discussed tendency to agglomerate in the polymer matrix when they are present in a higher quantity.

On the other hand, the two types of elongated hematite particles embedded in LDPE matrix, ellipsoid-shaped and peanut-shaped, enhance the material and improve the mechanical properties (tensile strength and elongation at break) in all studied contents. It is very important to say that the lowest content (0.25%) of hematite in LDPE has an extremely good influence on the mechanical properties of the composites for all studied elongated hematite particles of different shapes.

Compared to the values obtained for elongation at break in our previous work [15], it can be concluded that the highest values were obtained for the composites from the

previous work in which pseudocubic particles were used in a content of 0.5 and 1%. In contrast, for the content of 0.25%, composites with all elongated particles in this work show higher values for elongation at break than the composite with pseudocubic particles in the past work (LDPE/0.25%HC2).

Finally, it can be concluded that LDPE/hematite composites prepared in this work have potential to be used as packaging materials, especially as wrapping foils due to the high values of elongation at break.

### 3.4. Thermogravimetric Analysis (TGA)

The final properties of the polymer composites are highly influenced by the interactions of a polymer matrix and a metal oxide. It is very important to obtain a metal oxide's homogenous dispersion in a polymer, which improves the adhesion between them and improves the composite's properties. Distribution of a metal oxide in a polymer matrix is influenced by the metal oxide's size, shape, surface area, quantity and preparation conditions. Therefore, a specific combination of polymer matrix and metal oxides in polymer composites, depending on design parameters of the material, may contribute to an increase in the material's thermal stability, thermal conductivity and flame retardancy [34].

In this work, the thermal stability of LDPE/hematite composites, prepared with three types of elongated hematite particles, is studied by thermogravimetric analysis (TGA) and the results are presented in Table 3 and in Figure 7. Table 3 shows the values for the initial decomposition temperature ( $T_{95\%}$ ) and the temperature of the maximum rate of decomposition ( $T_{max}$ ). The thermal stability of LDPE/hematite composites is compared with the thermal stability of pure LDPE. From the results for  $T_{max}$ , it can be seen that the thermal decomposition of LDPE in the presence of all used elongated hematite particles is shifted towards higher temperatures. It is necessary to point out that even very low content of hematite particles (0.25%) causes an improvement of thermal stability. The highest thermal stability is observed for LDPE/0.5%HE2 composite, prepared with ellipsoidal particles, where the start of the decomposition ( $T_{95\%}$ ) is shifted to the higher temperature for 18 °C and the value for  $T_{max}$  is for more than 23 °C higher than the value for pure LDPE. The obtained high thermal stability of LDPE/0.5%HE2 composite is similar to the thermal properties from our previous work [15] obtained for LDPE/hematite composites with pseudocubic particles which showed the highest thermal stability of all LDPE/hematite composites studied in that work [15].

**Table 3.** The initial decomposition temperature ( $T_{95\%}$ ) and the temperature of the maximum rate of decomposition ( $T_{max}$ ).

Sample	$T_{95\%}$ (°C)	$T_{max}$ (°C)
LDPE	422.60	467.07
LDPE/0.25%HE2	416.23	486.07
LDPE/0.5%HE2	440.95	490.29
LDPE/1%HE2	438.83	483.01
LDPE/0.25%HP1	433.54	481.04
LDPE/0.5%HP1	434.99	479.67
LDPE/1%HP1	432.58	482.85
LDPE/0.25%HR1	428.93	475.92
LDPE/0.5%HR1	428.45	474.43
LDPE/1%HR1	429.60	474.75

These results indicate the strong influence of the used hematite particles on the thermal stability of polymer composites. This situation may be explained by a slower diffusion of volatile products of decomposition through the polymer due to the presence of filler particles [35]. The improved thermal stability of the composites with hematite filler can be also explained by the reduced mobility of the polymer chains due to their adsorption onto the surface of filler particles [9].

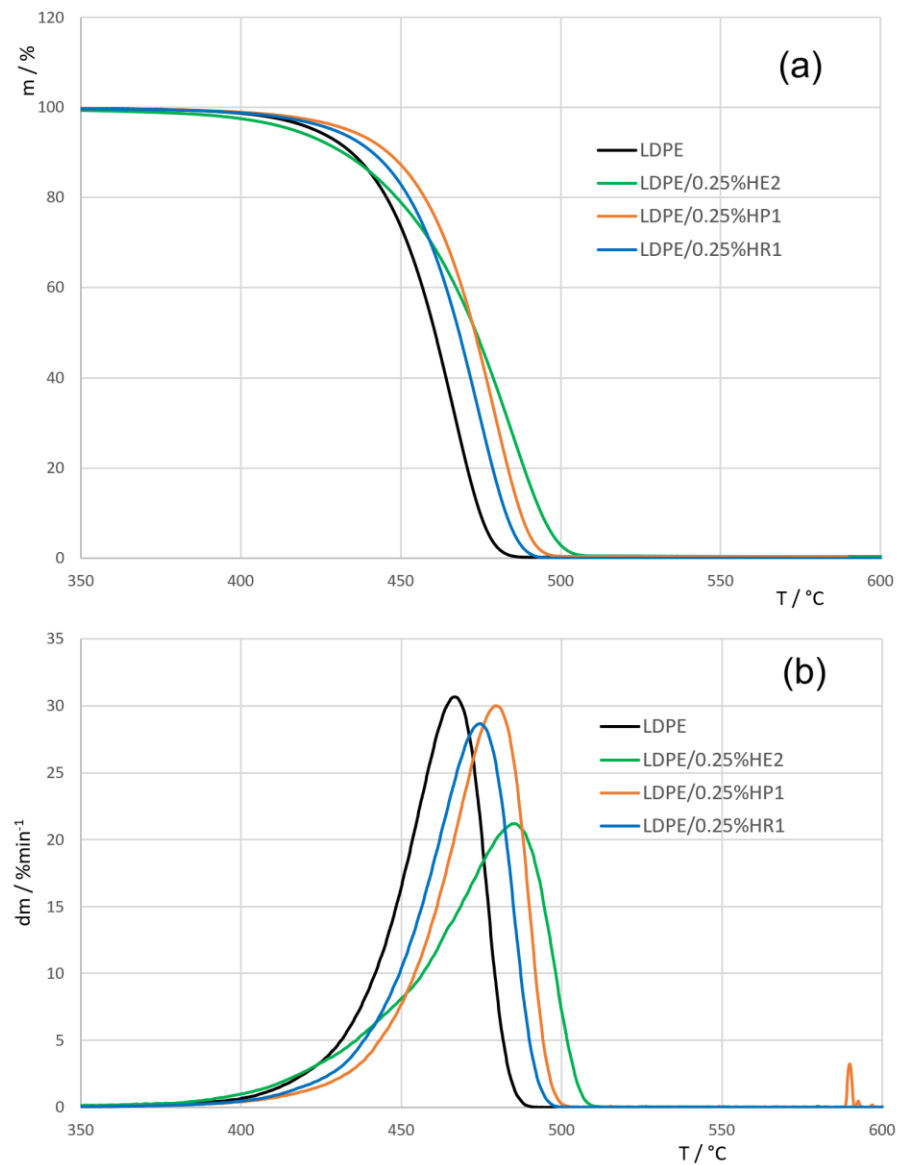


**Figure 7.** Thermogravimetric analysis (a) and differential thermogravimetric analysis (b) of LDPE/hematite composites containing 0.25 wt.% hematite particles of different shapes.

Rod-shaped hematite particles (R1) also show the influence on the improvement of the polymer composite's thermal stability but with less impact, due to their tendency to agglomerate in a polymer matrix [30]. They are long and straight particles with the highest tendency to agglomerate. Such metal oxide agglomeration, due to the high surface energy, decreases the adhesion of its particles to the polymer matrix and influences the final material properties [34].

### 3.5. Barrier Properties

In order to prolong the shelf-life and to maintain the quality of the products stored in polymer packaging, it is necessary to use polymer materials with improved barrier properties [36,37]. For example, during the storage of fresh meat, cheese, fruit and vegetables, moisture may be lost through the polymer packaging (in the form of foils and bags etc.), which leads to drying of the food and loss of its quality. The incorporation of well-dispersed fillers, like platelets or elongated particles, into a polymer matrix may significantly improve the barrier properties of the material and increase the diffusion path

of vapors and gases through it [38]. Figure 8 presents the results for barrier property, i.e., water vapor permeability, for LDPE and LDPE/hematite composites.

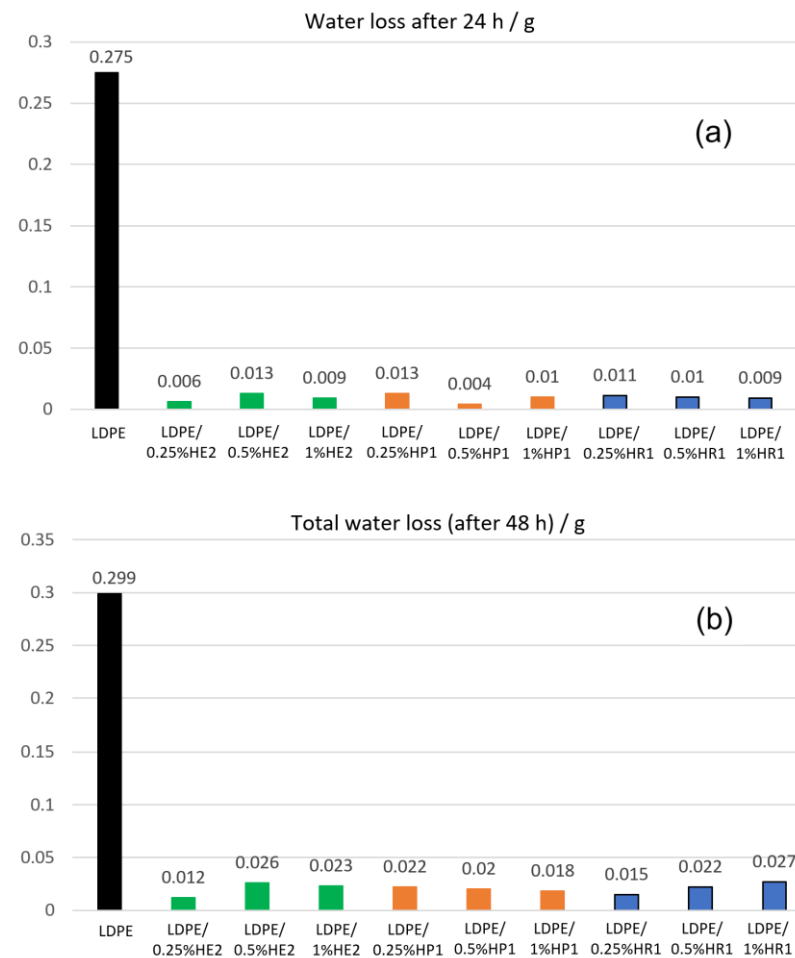


**Figure 8.** Water loss measured for prepared LDPE/hematite composites after 24 h (a) or 48 h (b).

The results show that all the prepared LDPE/hematite composites have noticeably lower water permeability than the neat polymer LDPE, which could be a consequence of the presence of hematite filler in the LDPE matrix. The present filler absorbs water and acts as a barrier to water loss due to the tortuosity path. It is known that this tortuosity is the main mechanism used to explain the decrease in permeability in polymer composites. Filler particles that are oriented and placed vertically to the permeation stream of the gases and vapors have more influence on the permeability decrease than filler particles which are unoriented. The effect of orientation may be noticed for elongated particles [38]. From the results in Figure 8, it is observed that all prepared composites, with all used types of elongated hematite particles and with every used hematite content (0.25%, 0.5% and 1%), show excellent resistance to water loss. For example, the sample LDPE/0.5%HP1 lost only 0.004 g of water after 24 h compared to the pure polymer LDPE, which lost 0.275 g of water during the same time period. Our work presents the results for the composites with very low filler content where the maximal filler loading was 1%. From the studied literature, it is known that there is decrease in permeability of the composites prepared with low filler loading due to its effectiveness in forming an impermeable crystalline phase. On the other hand, the higher nanofiller contents may show an increase in the water vapor permeability due to the effect of particle agglomeration [37]. Furthermore, the total water loss, after the 48 h, is still very low compared to the value obtained for pure LDPE.

It is worth mentioning that the obtained results are similar or better than the barrier properties for the best composite sample in our previous work [15], which is an LDPE/hematite composite with pseudocubic particles (LDPE/1%HC2).

It may be concluded that all the studied LDPE/hematite composites provide adequate protection to the water loss from the polymer packaging and can be considered as effective materials for packaging of wet products.

### 3.6. UV-Vis-NIR Spectroscopy

The new advanced polymer materials have unique properties, which make them usable in specific applications when there is a need for better durability and functionality. Among them, there is a group of materials with UV-blocking characteristics. Therefore, for successful protection from harmful UV radiation, there is a need for finding material formulations with UV resistance. UV protective agents, which are used alone or as fillers for polymer material, may be organic or inorganic. Inorganic components usually include different types of metal oxides like zinc oxide or titanium dioxide. When they are incorporated in polymer matrix at a certain content, polymer materials with the property of UV-blocking are formed [36,39].

It is known that inorganic UV filters filter the UV light by two mechanisms: absorption and Rayleigh diffusion [40]. Among the well-known inorganic substances for such applications, such as TiO<sub>2</sub> and ZnO, there is also iron oxide hematite [40], which starts to absorb radiation in the visible spectrum, in its green part, and strongly absorbs radiation of higher energy (UV radiation). Strong absorption of hematite in the UV range was attributed to the O 2p → Fe 3d charge transfer [40,41]. The absorption of UV and visible radiation (UV-Vis absorption spectrum) by hematite strongly depends on the particle size [41,42] but also on the particle shape [43–45] and doping [46–49]. The energy of the band gap for hematite is determined by the position of the absorption edge in the UV-Vis absorption spectrum and for bulk hematite is about 2.2 eV [50] but can be significantly higher for very small (nano-size) hematite particles [41,42] or lower, as in the case of some doped hematite samples [46–49].

The UV-Vis-NIR diffuse reflectance spectra of pure LDPE and LDPE/hematite composites with hematite particles (ellipsoids, rods and peanuts) content of 1%, 0.5% and 0.25% are shown in Figure 9 (a–c, respectively). The spectra of all LDPE/hematite composites showed a much higher absorption intensity in the UV and part of the visible region compared to the spectrum of pure LDPE. The highest absorption in the UV range was shown by LDPE/hematite composites with ellipsoidal hematite particles (HE2), for all three mass fractions of hematite particles. Although the absorption of UV and visible light decreased with decreasing hematite content, LDPE/hematite composites with ellipsoidal hematite particles showed quite strong absorption even for the lowest hematite content (0.25%). Very good absorption of UV and visible radiation was also shown by LDPE/hematite composites with rod-shaped hematite particles (HR1), while LDPE/hematite composites with peanut-shaped hematite particles (HP1) showed significantly lower absorption, especially for the lowest content of HP1 particles (0.25%). For good UV protection of the composites with peanut-shaped hematite particles, a significantly higher mass fraction of hematite particles is needed (1%) compared to ellipsoidal or rod-shaped hematite particles, for which even a mass fraction of 0.25% is sufficient for very good protection against UV radiation.

In our previous work [15], the highest absorption intensity of UV light was observed for composites prepared with spherical hematite particles (LDPE/HS1). The determined value for LDPE/1%HS1 sample is quite similar to the value of LDPE/1%HE2 sample in the current study. On the other hand, the samples with lower hematite content (LDPE/0.5%HE2 and LDPE/0.25%HE2) from the present study show stronger UV absorption than the samples LDPE/0.5%HS1 and LDPE/0.25%HS1 from the past work.

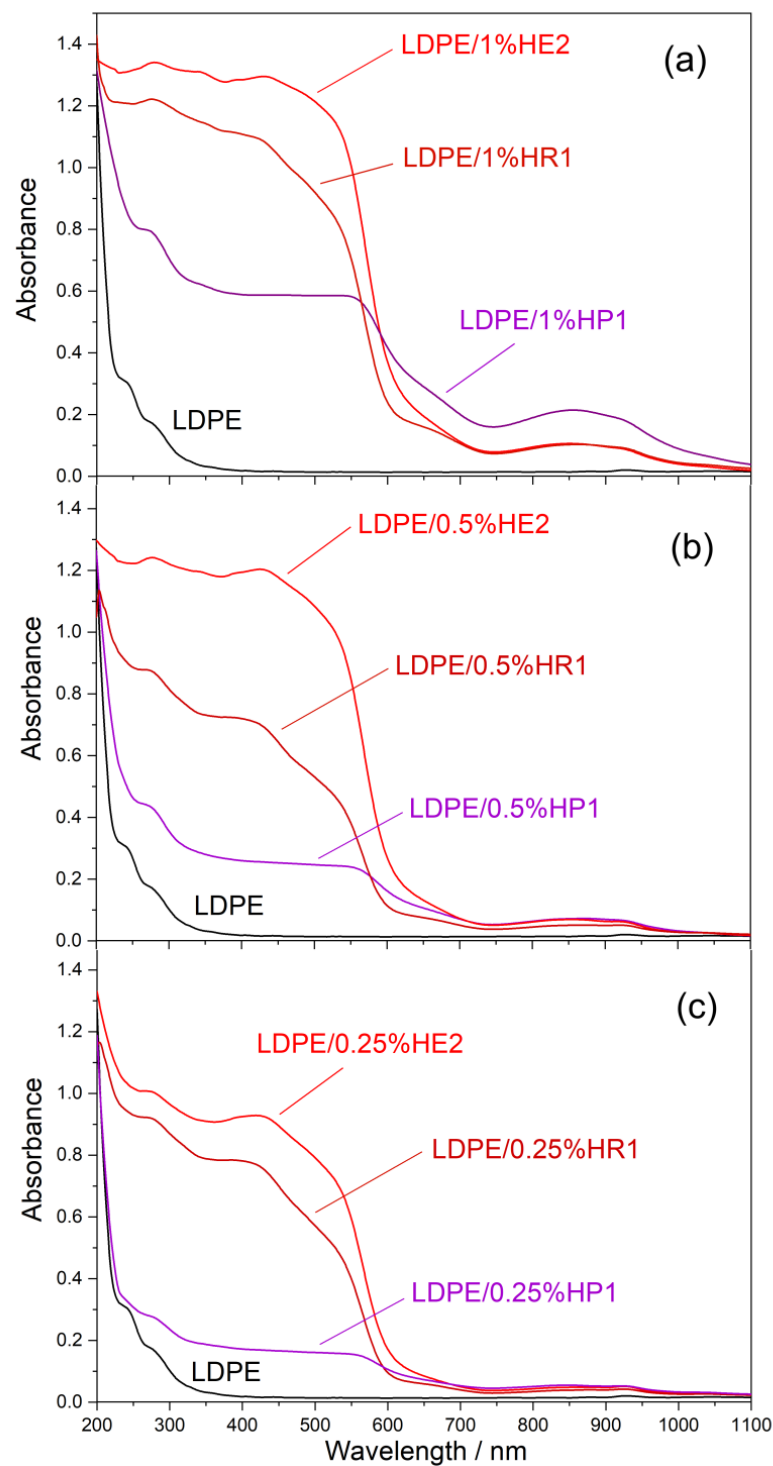


**Figure 9.** UV-Vis-NIR diffuse reflectance spectra of prepared LDPE/hematite composites containing 1 wt.% (a), 0.5 wt.% (b) or 0.25 wt.% (c) hematite.

It can be concluded that all prepared LDPE/hematite composites have great potential to be used as advanced polymer materials with UV-blocking ability. The ultraviolet shielding mechanism of LDPE/hematite composites is presented in Figure 10. In general, such composites may be declared as functional polymer materials with protective properties to UV-light degradation.

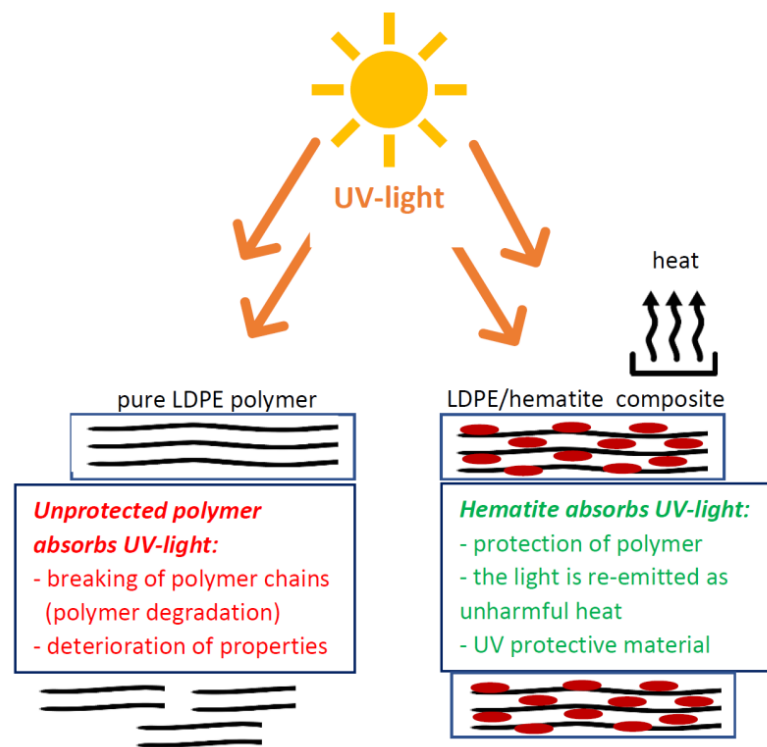


Figure 10. The ultraviolet shielding mechanism of LDPE/hematite composites.

#### 4. Conclusions

This study presents LDPE/hematite composites prepared with hydrothermally synthesized, well-defined and fairly uniform elongated hematite particles of different shapes, ellipsoidal, peanut-shaped and rod-shaped, at a content of 0.25 wt.%, 0.5 wt.% and 1 wt.% in an LDPE matrix. The results show that all prepared LDPE/hematite composites have improved thermal, mechanical, barrier and UV-blocking properties compared to the neat LDPE.

The lowest content (0.25%) of hematite in polymer composites causes an improvement of the mechanical properties for all studied hematite particles. Furthermore, ellipsoidal and peanut-shaped hematite particles cause an increase in the tensile strength and elongation at break of the composites prepared with all studied contents (0.25%, 0.5% and 1%). Incorporated rod-shaped hematite particles cause a decrease in elongation at break compared to the neat LDPE, when present in higher quantities (0.5% and 1%), which is attributed to their tendency to agglomerate. The thermal stability of LDPE/hematite composites is enhanced by the use of all types and all mass fractions of elongated hematite particles. Furthermore, all prepared composites provide a good barrier property, i.e., protection against water loss. LDPE/hematite composites with ellipsoidal and rod-shaped hematite particles show good UV protection even for very low hematite content (0.25%), while the composites with peanut-shaped hematite particles need a higher content of hematite particles (1%) for adequate UV protection.

It can be concluded that the composites prepared with ellipsoidal hematite particles (LDPE/HE2) have the best comprehensive performance due to their very good thermal properties and UV absorption ability as well as improved mechanical and barrier properties in comparison to pure LDPE polymer.

On the basis of the obtained results, it can be concluded that LDPE/hematite composites are materials with good potential for application as polymer packaging with enhanced mechanical, thermal, barrier and UV-protective properties.

**Author Contributions:** Conceptualization, L.K.K.; methodology, L.K.K.; validation, L.K.K., A.P. and S.K.; investigation, L.K.K., A.P., N.P. and S.K.; resources, L.K.K. and S.K.; data curation, L.K.K., A.P. and S.K.; writing—original draft preparation, L.K.K. and S.K.; writing—review and editing, L.K.K. and S.K.; visualization, L.K.K., A.P. and S.K.; supervision, L.K.K. and S.K.; project administration, S.K.; funding acquisition, L.K.K. and S.K. All authors have read and agreed to the published version of the manuscript.

**Funding:** This research was partially funded by the Croatian Science Foundation, project number IP-2016-06-8254.

**Data Availability Statement:** The data that support the findings of this study are available from the corresponding author (L.K.K.) upon reasonable request.

**Acknowledgments:** The authors thank Mirela Leskovic, Faculty of Chemical Engineering and Technology, University of Zagreb, for the availability of mechanical measurements.

**Conflicts of Interest:** The authors declare no conflicts of interest.

## References

1. Gerstle, F.P. Composites. In *Encyclopedia of Polymer Science and Technology*, 2nd ed.; Mark, H.F., Bikales, N.M., Overberger, C.G., Menges, G., Eds.; J. Wiley & Sons: New York, NY, USA, 1985; Volume 6, pp. 776–820.
2. Rotheron, R.N. (Ed.) *Particulate-Filled Polymer Composites*; Rapra Technology Limited: Shawbury, UK, 2003.
3. Rotheron, R. (Ed.) *Fillers for Polymer Applications*; Springer International Publishing: Cham, Switzerland, 2017.
4. Siva Prasanna, S.R.V.; Balaji, K.; Pandey, S.; Rana, S. Metal Oxide Based Nanomaterials and Their Polymer Nanocomposites. In *Nanomaterials and Polymer Nanocomposites*, 1st ed.; Karak, N., Ed.; Elsevier: Amsterdam, The Netherlands, 2019; pp. 123–144.
5. Yadav, R.; Singh, M.; Shekhawat, D.; Lee, S.-Y.; Park, S.-J. The role of fillers to enhance the mechanical, thermal, and wear characteristics of polymer composite materials: A review. *Compos. Part A Appl. Sci. Manuf.* **2023**, *175*, 107775. [[CrossRef](#)]
6. Sahu, S.K.; Boggarapu, V.; Sreekanth, P.S.R. Improvements in the mechanical and thermal characteristics of polymer matrix composites reinforced with various nanofillers: A brief review. *Mater. Today Proc.* **2023**, *in press*. [[CrossRef](#)]
7. Kausar, A. Polymeric materials filled with hematite nanoparticle: Current state and prospective application. *Polym. Plast. Technol. Mater.* **2020**, *59*, 323–338. [[CrossRef](#)]
8. Djoković, V.; Nedeljković, J.M. Stress relaxation in hematite nanoparticles-polystyrene composites. *Macromol. Rapid Commun.* **2000**, *21*, 994–997. [[CrossRef](#)]
9. Marinović-Cincović, M.; Šaponjić, Z.V.; Djoković, V.; Milonjić, S.K.; Nedeljković, J.M. The influence of hematite nano-crystals on the thermal stability of polystyrene. *Polym. Degrad. Stab.* **2006**, *91*, 313–316. [[CrossRef](#)]
10. Greenstein, K.E.; Myung, N.V.; Parkin, G.F.; Cwiertny, D.M. Performance comparison of hematite ( $\alpha$ -Fe<sub>2</sub>O<sub>3</sub>)-polymer composite and core-shell nanofibers as point-of-use filtration platforms for metal sequestration. *Water Res.* **2019**, *148*, 492–503. [[CrossRef](#)]
11. Mensah, E.E.; Abbas, Z.; Azis, R.S.; Ibrahim, N.A.; Khamis, A.M.; Abdalhadhi, D.M. Complex permittivity and power loss characteristics of  $\alpha$ -Fe<sub>2</sub>O<sub>3</sub>/polycaprolactone (PCL) nanocomposites: Effect of recycled  $\alpha$ -Fe<sub>2</sub>O<sub>3</sub> nanofiller. *Heliyon* **2020**, *6*, e05595. [[CrossRef](#)] [[PubMed](#)]
12. Bora, M.A.; Adhav, P.B.; Diwate, B.B.; Pawar, D.S.; Dallavalle, S.; Chabukswar, V.V. Room temperature operating sensitive and reproducible ammonia sensor based on PANI/hematite nanocomposite. *Polym. Plast. Technol. Mater.* **2019**, *58*, 1545–1555. [[CrossRef](#)]
13. Matysiak, W.; Tański, T.; Zaborowska, M. Electrospinning process and characterization of PVP/hematite nanofibers. *IOP Conf. Ser. Mater. Sci. Eng.* **2019**, *461*, 012050. [[CrossRef](#)]
14. Palimi, M.J.; Rostami, M.; Mahdavian, M.; Ramezanzadeh, B. A study on the corrosion inhibition properties of silane-modified Fe<sub>2</sub>O<sub>3</sub> nanoparticle on mild steel and its effect on the anticorrosion properties of the polyurethane coating. *J. Coat. Technol. Res.* **2015**, *12*, 277–292. [[CrossRef](#)]
15. Peršić, A.; Popov, N.; Kratožil Krehula, L.; Krehula, S. The Influence of Different Hematite ( $\alpha$ -Fe<sub>2</sub>O<sub>3</sub>) Particles on the Thermal, Optical, Mechanical, and Barrier Properties of LDPE/Hematite Composites. *Materials* **2023**, *16*, 706. [[CrossRef](#)] [[PubMed](#)]
16. Lin, Y.-M.; Abel, P.R.; Heller, A.; Mullins, C.B.  $\alpha$ -Fe<sub>2</sub>O<sub>3</sub> Nanorods as Anode Material for Lithium Ion Batteries. *J. Phys. Chem. Lett.* **2011**, *2*, 2885–2891. [[CrossRef](#)]
17. Liu, X.; Liu, J.; Chang, Z.; Sun, X.; Li, Y. Crystal plane effect of Fe<sub>2</sub>O<sub>3</sub> with various morphologies on CO catalytic oxidation. *Catal. Commun.* **2011**, *12*, 530–534. [[CrossRef](#)]
18. Zhou, X.; Lan, J.; Liu, G.; Deng, K.; Yang, Y.; Nie, G.; Yu, J.; Zhi, L. Facet-Mediated Photodegradation of Organic Dye over Hematite Architectures by Visible Light. *Angew. Chem. Int. Ed.* **2012**, *51*, 178–182. [[CrossRef](#)]
19. Kment, S.; Riboni, F.; Pausova, S.; Wang, L.; Wang, L.; Han, H.; Hubicka, Z.; Krysa, J.; Schmuki, P.; Zboril, R. Photoanodes based on TiO<sub>2</sub> and  $\alpha$ -Fe<sub>2</sub>O<sub>3</sub> for solar water splitting—Superior role of 1D nanoarchitectures and of combined heterostructures. *Chem. Soc. Rev.* **2017**, *46*, 3716–3769. [[CrossRef](#)]
20. Hore, M.J.A.; Composto, R.J. Functional Polymer Nanocomposites Enhanced by Nanorods. *Macromolecules* **2014**, *47*, 875–887. [[CrossRef](#)]

21. Li, Z.; Lai, X.; Wang, H.; Mao, D.; Xing, C.; Wang, D. Direct hydrothermal synthesis of single-crystalline hematite nanorods assisted by 1,2-propanediamine. *Nanotechnology* **2009**, *20*, 245603. [[CrossRef](#)]
22. Sugimoto, T.; Khan, M.M.; Muramatsu, A. Preparation of monodisperse peanut-type  $\alpha$ -Fe<sub>2</sub>O<sub>3</sub> particles from condensed ferric hydroxide gel. *Colloids Surf. A Physicochem. Eng.* **1993**, *70*, 167–169. [[CrossRef](#)]
23. Klug, H.P.; Alexander, L.E. *X-ray Diffraction Procedures*; John Wiley & Sons: New York, NY, USA, 1974; p. 687.
24. Gulmine, J.V.; Janissek, J.V.; Heise, H.M.; Akcelrud, L. Polyethylene characterization by FTIR. *Polym. Test.* **2002**, *21*, 557–563. [[CrossRef](#)]
25. Chao, Y.; Jianming, Z.; Deyan, S.; Shouke, Y. Structure characterization of melt drawn polyethylene ultrathin films. *Chin. Sci. Bull.* **2006**, *51*, 2844–2850.
26. Wang, Y.; Muramatsu, A.; Sugimoto, T. FTIR analysis of well-defined  $\alpha$ -Fe<sub>2</sub>O<sub>3</sub> particles. *Colloids Surf. A Physicochem. Eng. Asp.* **1998**, *134*, 281–297. [[CrossRef](#)]
27. Fernando, S.S.; Christensen, P.A.; Egerton, T.A.; White, J.R. Carbon dioxide evolution and carbonyl group development during photodegradation of polyethylene and polypropylene. *Polym. Degrad. Stab.* **2007**, *92*, 2163–2172. [[CrossRef](#)]
28. Dudić, D.; Marinović-Cincović, M.; Nedeljković, J.M.; Djokovic, V. Electrical properties of a composite comprising epoxy resin and  $\alpha$ -hematite nanorods. *Polymer* **2008**, *49*, 4000–4008. [[CrossRef](#)]
29. Fu, S.-Y.; Feng, X.-Q.; Lauke, B.; Mai, Y.-W. Effects of particle size, particle/matrix interface adhesion and particle loading on mechanical properties of particulate–polymer composites. *Compos. B Eng.* **2008**, *39*, 933–961. [[CrossRef](#)]
30. Bogdanović, G.; Kovač, T.S.; Džunuzović, E.S.; Špírková, M.; Ahrenkiel, P.S.; Nedeljković, J.M. Influence of hematite nanorods on the mechanical properties of epoxy resin. *J. Serbian Chem. Soc.* **2017**, *82*, 437–447. [[CrossRef](#)]
31. Huang, D.; Zhang, Z.; Ma, Z.; Quan, Q. Effect of Natural Nanostructured Rods and Platelets on Mechanical and Water Resistance Properties of Alginate-Based Nanocomposites. *Front. Chem.* **2018**, *6*, 635. [[CrossRef](#)] [[PubMed](#)]
32. Caseri, W.R. Nanocomposites of polymers and inorganic particles: Preparation, structure and properties. *Mater. Sci. Technol.* **2006**, *22*, 807–817. [[CrossRef](#)]
33. Pracella, M.; Rolla, L.; Chionna, D.; Galeski, A. Compatibilization and properties of poly(ethylene terephthalate)/polyethylene blends based on recycled materials. *Macromol. Chem. Phys.* **2002**, *203*, 1473–1485. [[CrossRef](#)]
34. Kaya, G.G.; Deveci, H. Design and synthesis of metal oxide–polymer composites. In *Renewable Polymers and Polymer-Metal Oxide Composites: Synthesis, Properties, and Applications*, 1st ed.; Haider, S., Haider, A., Eds.; Elsevier: Amsterdam, The Netherlands, 2022; pp. 101–128.
35. Silvestre, C.; Duraccio, D.; Cimmino, S. Food packaging based on polymer nanomaterials. *Prog. Polym. Sci.* **2011**, *36*, 1766–1782. [[CrossRef](#)]
36. Hrnjak Murgić, Z.; Rešček, A.; Ptiček Siročić, A.; Kratofil Krehula, L.; Katančić, Z. *Nanoparticles in Active Polymer Food Packaging*; Smithers Pira Technology Ltd.: Shawbury, UK, 2015.
37. Kausar, A. A review of high-performance polymer nanocomposites for packaging applications in electronics and food industries. *J. Plast. Film Sheeting* **2020**, *36*, 94–112. [[CrossRef](#)]
38. Wolf, C.; Angellier-Coussy, H.; Gontard, N.; Doghieri, F.; Guillard, V. How the shape of fillers affects the barrier properties of polymer/non-porous particles nanocomposites: A review. *J. Membr. Sci.* **2018**, *556*, 393–418. [[CrossRef](#)]
39. He, J.; Shao, W.; Zhang, L.; Deng, C.; Li, C. Crystallization behavior and UV-protection property of PET-ZnO nanocomposites prepared by in situ polymerization. *J. Appl. Polym. Sci.* **2009**, *114*, 1303–1311. [[CrossRef](#)]
40. Truffault, L.; Choquet, B.; Konstantinov, K.; Devers, T.; Couteau, C.; Coiffard, L.J.M. Synthesis of nano-hematite for possible use in sunscreens. *J. Nanosci. Nanotechnol.* **2011**, *11*, 2413–2420. [[CrossRef](#)]
41. Chernyshova, I.V.; Ponnurangam, S.; Somasundaran, P. On the origin of an unusual dependence of (bio)chemical reactivity of ferric hydroxides on nanoparticle size. *Phys. Chem. Chem. Phys.* **2010**, *12*, 14045–14056. [[CrossRef](#)]
42. Schwaminger, S.P.; Surya, R.; Filser, S.; Wimmer, A.; Weigl, F.; Fraga-García, P.; Berensmeier, S. Formation of iron oxide nanoparticles for the photooxidation of water: Alteration of finite size effects from ferrihydrite to hematite. *Sci. Rep.* **2017**, *7*, 12609. [[CrossRef](#)] [[PubMed](#)]
43. Lian, J.; Duan, X.; Ma, J.; Peng, P.; Kim, T.; Zheng, W. Hematite ( $\alpha$ -Fe<sub>2</sub>O<sub>3</sub>) with Various Morphologies: Ionic Liquid-Assisted Synthesis, Formation Mechanism, and Properties. *ACS Nano* **2009**, *3*, 3749–3761. [[CrossRef](#)]
44. Zhang, X.; Niu, Y.; Li, Y.; Hou, X.; Wang, Y.; Bai, R.; Zhao, J. Synthesis, optical and magnetic properties of  $\alpha$ -Fe<sub>2</sub>O<sub>3</sub> nanoparticles with various shapes. *Mater. Lett.* **2013**, *99*, 111–114. [[CrossRef](#)]
45. Wang, T.; Zhou, S.; Zhang, C.; Lian, J.; Liang, Y.; Yuan, W. Facile synthesis of hematite nanoparticles and nanocubes and their shape-dependent optical properties. *New J. Chem.* **2014**, *38*, 46–49. [[CrossRef](#)]
46. Popov, N.; Krehula, S.; Ristić, M.; Kuzmann, E.; Homonnay, Z.; Bošković, M.; Stanković, D.; Kubuki, S.; Musić, S. Influence of Cr doping on the structural, magnetic, optical and photocatalytic properties of  $\alpha$ -Fe<sub>2</sub>O<sub>3</sub> nanorods. *J. Phys. Chem. Solids* **2021**, *148*, 109699. [[CrossRef](#)]
47. Popov, N.; Bošković, M.; Perović, M.; Nemeth, Z.; Wang, J.; Kuang, Z.; Reissner, M.; Kuzmann, E.; Homonnay, Z.; Kubuki, S.; et al. Influence of low-spin Co<sup>3+</sup> for high-spin Fe<sup>3+</sup> substitution on the structural, magnetic, optical and catalytic properties of hematite ( $\alpha$ -Fe<sub>2</sub>O<sub>3</sub>) nanorods. *J. Phys. Chem. Solids* **2021**, *152*, 109929. [[CrossRef](#)]

48. Popov, N.; Bošković, M.; Perović, M.; Zadro, K.; Gilja, V.; Kratofil Krehula, L.; Robić, M.; Marciuš, M.; Ristić, M.; Musić, S.; et al. Effect of Ru<sup>3+</sup> ions on the formation, structural, magnetic and optical properties of hematite ( $\alpha$ -Fe<sub>2</sub>O<sub>3</sub>) nanorods. *J. Magn. Magn. Mater.* **2021**, *538*, 16831. [[CrossRef](#)]
49. Popov, N.; Ristić, M.; Bošković, M.; Perović, M.; Marciuš, M.; Stanković, D.; Krehula, S. Influence of Sn doping on the structural, magnetic, optical and photocatalytic properties of hematite ( $\alpha$ -Fe<sub>2</sub>O<sub>3</sub>) nanoparticles. *J. Phys. Chem. Solids* **2022**, *161*, 110372. [[CrossRef](#)]
50. Cornell, R.M.; Schwertmann, U. *The Iron Oxides-Structure, Properties, Reactions, Occurrence and Uses*, 2nd ed.; Wiley-VCH: Weinheim, Germany, 2003.

**Disclaimer/Publisher's Note:** The statements, opinions and data contained in all publications are solely those of the individual author(s) and contributor(s) and not of MDPI and/or the editor(s). MDPI and/or the editor(s) disclaim responsibility for any injury to people or property resulting from any ideas, methods, instructions or products referred to in the content.